J Fluoresc (2013) 23:1121–1138
DOI 10.1007/s10895-013-1241-7

ORIGINAL PAPER

TDDFT Investigation of the Electronic Structures and Photophysical Properties of Fluorescent Extended Styryl Push-Pull Chromophores Containing Carbazole Unit

Vinod D. Gupta · Abhinav B. Tathe · Vikas S. Padalkar · Vikas S. Patil · Kiran R. Phatangare · Prashant G. Umape · Ponnadurai Ramasami · Nagaiyan Sekar

Received: 7 February 2013 / Accepted: 22 May 2013 / Published online: 11 June 2013

Abstract Push-pull chromophores attached to carbazole based π-conjugating spacers bearing *N*-alkylamino donors, cyanovinyl and carbethoxy acceptors have been studied by the means of UV-Visible measurements. The intramolecular charge transfer (ICT) of these π-conjugated systems has also been tested by investigating the ability of the solute molecules to undergo shifts in their fluorescence emission maxima with increasing solvent polarity. Density Functional Theory [B3LYP/6-31G(d)] and Time Dependent Density Functional Theory [TD-B3LYP/6-31G(d)] computations have been used to have more understanding of the structural, molecular, electronic and photophysical parameters of push-pull dyes. The largest wavelength difference between the experimental and computed electronic absorption maxima was 45 nm. For emission, a largest difference of 61 nm was observed. The ground state and excited state dipole moments in different solvents were determined using experimental solvatochromic data and computed Onsager radii. The dipole moments of the molecules in the excited state were observed to be higher than in the ground state.

Keywords Carbazole · Density functional calculation · TDDFT · Dipole moment · Fluorescent styryl dyes · Solvatochromism

Electronic supplementary material The online version of this article (doi:10.1007/s10895-013-1241-7) contains supplementary material, which is available to authorized users.

V. D. Gupta · A. B. Tathe · V. S. Padalkar · V. S. Patil · K. R. Phatangare · P. G. Umape · N. Sekar (✉)
Tinctorial Chemistry Group, Department of Dyestuff Technology, Institute of Chemical Technology, N. P. Marg, Matunga, Mumbai 400 019 Maharashtra, India
e-mail: n.sekar@ictmumbai.edu.in

N. Sekar
e-mail: nethi.sekar@gmail.com

V. D. Gupta · P. Ramasami (✉)
Computational Chemistry Group, Faculty of Science, Department of Chemistry, University of Mauritius, Réduit, Mauritius
e-mail: ramchemi@intnet.mu

Introduction

In recent years, electroluminescent [1, 2], photoluminescent [3] and nonlinear optical materials [4–6] have attracted great attention due to their possible utilization in electro-optical display devices. There is an increasing demand for such type of high-performance materials particularly multi-functional opto-electronic materials. Such kinds of materials have invariably fluorescent properties. Among several fluorescent materials, organic fluorophores have the advantages of tunability and high intensity of absorption and emission combined with high thermal stability [7]. Electroluminescence (EL) efficiency of OLEDs can be improved by using good emitters with bipolar charge transport properties [8]. The fluorophores possessing donor–acceptor (D-A) framework have been widely applied, but the large dipole moment of these molecules usually leads to fluorescence quenching [9–11].

The organic fluorophores usually contain electron donor–acceptor (D-A) groups separated by extensive π-conjugation in a heteroaromatic system. Carbazole happens to be one of the interesting heterocyclic units occurring in fluorescent colorants [12]. They have been studied widely because of their large π-electron conjugation and strong intramolecular

electron transfer characteristics. Carbazole derivatives are also important as hole-transporting materials between the emitting layer and the anode to balance the charge injection [13]. The molecular functional properties of carbazole can be favourably manipulated by functionalizing at 3-, 6- and/or 9-positions [14].

For the last decade, research interests have been directed to synthesize push-pull chromophoric system with large higher-order nonlinear optical properties containing carbazole units [15–20]. Recently Panthi et al. reported that fluorescent organic nanoparticles made from carbazole compounds have large Stokes shift leading to emission in the NIR region [21]. Push-pull chromophore consists of a polar D-π-A system with a planar π-system attached to a strong electron donor and a strong electron acceptor on opposite side. Carbazole derivatives with D-π-A structures have, in general, a large electron delocalization length and the ability of experiencing intramolecular charge transfer (ICT) from the electron donating groups to electron accepting groups [22].

Theoretical computations have been used to have an in-depth understanding of functional properties like luminescence and hyperpolarizability at molecular level [23–25]. Density functional theory (DFT) [26, 27] based computational methods have advantages due to their well-defined electron correlation energies and low computational cost. Time dependant density functional theory (TDDFT) has become one of the important tools to understand the excited state configuration and electronic spectra of medium-sized and large molecules. Push-pull chromophoric systems have been studied using DFT methods in the recent years [28–30].

In continuation of our earlier work on the synthesis of carbazole containing D-π-A and A-π-D-π-A type of organic extended styryl dyes [31] and the synthesis of novel fluorescent molecules [32, 33], we hereby report further experimental investigation on solvatochromism, solvatofluorism, and quantum yields of dyes **5a**, **5b**, **6a** and **6b** (Fig. 1) in various solvents. Lippert-Mataga and related models [34–43] were used to derive the ground and excited states dipole moments. TDDFT based approach has been used to have more understanding of the geometry in the ground and excited states, photo-physical and non-linear properties of these four dyes.

Experimental Section

Materials and Equipments

All the commercial reagents and solvents were purchased from Sd Fine Chemicals Pvt. Ltd. and they were used without purification and all the solvents were of spectroscopic grade. The absorption spectra of the dyes were recorded on a Spectronic Genesys 2 UV-Visible spectrophotometer, and emission spectra were recorded on Varian Cary Eclipse fluorescence spectrophotometer using freshly prepared solutions in solvents of different polarities at the concentration of 1×10^{-6} mol L^{-1}. Dyes **5a**, **5b**, **6a** and **6b** were synthesized and purified as we reported previously [31]. Quantum yields were determined in different solvents by using Rhodamine B (Φ=0.97 in ethanol) [44] as a reference standard using the comparative method.

The photophysical properties were investigated using solvatochromic and solvatofluoric behaviours of the dyes. Solvatochromic data was used to determine the ground and excited state dipole moments of the dyes **5a**, **5b**, **6a** and **6b** by using Lippert-Mataga, Bakhshiev and Kawski-Chamma-Viallet correlations.

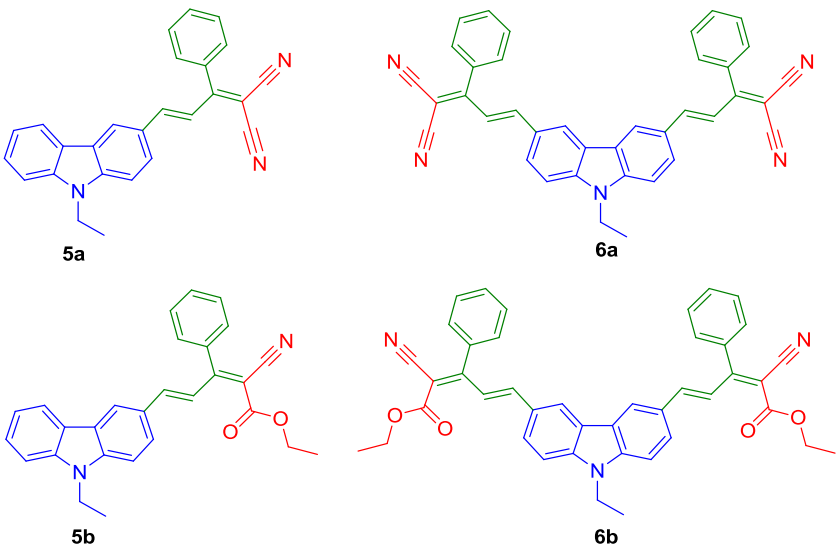

Fig. 1 Structures of the dyes **5a**, **5b**, **6a** and **6b**

Computational Details

All computations were performed using the Gaussian 09 program package [45]. The ground state (S_0) geometry of the reported dyes was optimized in the gas phase using DFT [46]. The functional used was B3LYP. The B3LYP method combines Becke's three parameter exchange functional (B3) [26] with the nonlocal correlation functional by Lee, Yang and Parr (LYP) [47]. The basis set used for all atoms was 6-31G(d). The vibrational frequencies at the optimized structures were computed using the same method to verify that the optimized structures correspond to local minima on the energy surface. The vertical excitation energies and oscillator strengths were obtained for the lowest 10 singlet-singlet transitions at the optimized ground state equilibrium geometries by using the Time Dependent Density Functional Theory (TDDFT) at the same hybrid functional and basis set [48–50].

The low-lying first singlet excited states (S_1) of the dyes were relaxed using the TDDFT to obtain their minimum energy geometries. The difference between the energies of the optimized geometries at the first singlet excited state and the ground state was used in calculating the emission [51]. Frequency computations were also carried out on Frank-Condon excited state of the dyes. All the computations in solvents of different polarities were carried out using the Self-Consistent Reaction Field (SCRF) under the Polarizable Continuum Model (PCM) [52, 53]. The electronic absorption spectra, including wavelengths, oscillators strengths, and main configuration assignment, were systematically investigated using TDDFT with PCM model on the basis of the optimized ground structures.

Results and Discussion

Optimized Geometries of Dyes

The ground state geometries of the dyes are having almost planar arrangement of the carbazole unit, π-bridge and acceptor group. While, phenyl ring on π -bridge unit is twisted. The resulting optimized geometry of dye **5a** is such that it has a small twist dihedral angle C_{10}-C_9-C_{33}-N_{35} as 12.3° (Fig. 2) but bis-styryl dye **6a** showed little lower twist of 12.0° (Figure S2). Dye **6a** has a vertical plane of symmetry. The bond length of mirror bonds like C_{28}-C_{29} and C_{44}-C_{45} are same in both ground state as well as in excited state (Figure S2).

The optimized geometry of dye **5b** is such that it has also a small twist dihedral angle of 16.1° along C_{10}-C_9-C_{33}-O_{35} angle between the carbazole ring and carbethoxy units (Figure S1). But the dye **6b** showed highest torsional angle among the four dyes of 29.1° (Figure S3). Also, the two carbonyl groups are facing away from the carbazole ring whereas in dye **5b**, the carbonyl groups are facing towards the carbazole ring. The pending phenyl ring on C_{30} atom was twisted with dihedral angles 64.0° and 63.3° in case of dyes **5b** and **6b** which are higher than those of dyes **5a** and **6a**.

In the excited state geometry, the major bond lengthening was observed between the bonds C_{28}-C_{29}, C_{30}-C_{31}, C_{32}-N_{34}, C_{33}-O_{35} and C_{33}-O_{44} by 0.020, 0.043, 0.005, 0.009 and 0.016 Å and bond length shortened for the bonds C_{29}-C_{30}, C_{31}-C_{32}, C_{31}-C_{33} by 0.012, 0.011, 0.023 Å for dye **5b** (Figure S1). Similarly for dye **6a**, the bonds C_{28}-C_{29}, C_{30}-C_{31},C_{32}-N_{34} and C_{33}-N_{35} were found to be lengthened by 0.016, 0.022, 0.003 and 0.003 Å, and bonds shortened at C_{29}-C_{30}, C_{31}-C_{32}, C_{31}-C_{33} by 0.013, 0.007, 0.007 Å (Figure S2). Similar behaviour was observed for dyes **5a** and **6b** (Figs. 2 and S3). Such lengthening and shortening of the bonds i.e. the bond length alteration were due to the effect of donor and acceptor groups present in the molecules.

The Mulliken charge distribution in ground and excited states on selected atoms of the dyes **5a**, **5b**, **6a** and **6b** are shown in Table 1 and Figures S3–S7. The increase in the positive charge on atom C_{30} in the excited state is due to phenyl ring which decreases the electron density at this carbon atom. This atom is also engaged in bond lengthening in the excited state along the bond C_{30}-C_{31}. The charge on nitrogen atom present in terminal cyano group increases which is a characteristic electron pulling effect of the cyano group. This increases the positive charge on atom C_{32} and decreases on carbon C_{31} suggesting extensive charge delocalization in the entire molecule. Structural diagrams of these dyes were visualized using CYLview software [54].

Solvatochromism and Solvatofluorism

Absorption and emission data for the dyes **5a**, **5b**, **6a** and **6b** measured in different solvents are shown in Tables 2 and 3 and Figs. 3, S8–S10. The red shifted absorption band (Table 2) of dye **5a** (Fig. 3) indicates that dicyanovinyl moiety has a stronger electron pulling effect than the cyanocarbethoxy vinyl unit (dye **5b**) which is responsible for the increase in the charge transfer between donors and acceptors in the case of dicyanovinylene dyes. In the case of dye **5b**, the absorption maxima remain fairly insensitive to solvent polarity whereas for the other three dyes **5a**, **6a** and **6b** slight variations in absorption maxima were observed indicating that emitting the excited state is more polar in character than the ground state. Emission maxima of these dyes were largely red shifted as the solvent polarity increases. It is to be noted that the solvent polarity has a strong influence on emission as well as quantum efficiency of a molecule. Dye **6b** showed higher quantum yield than

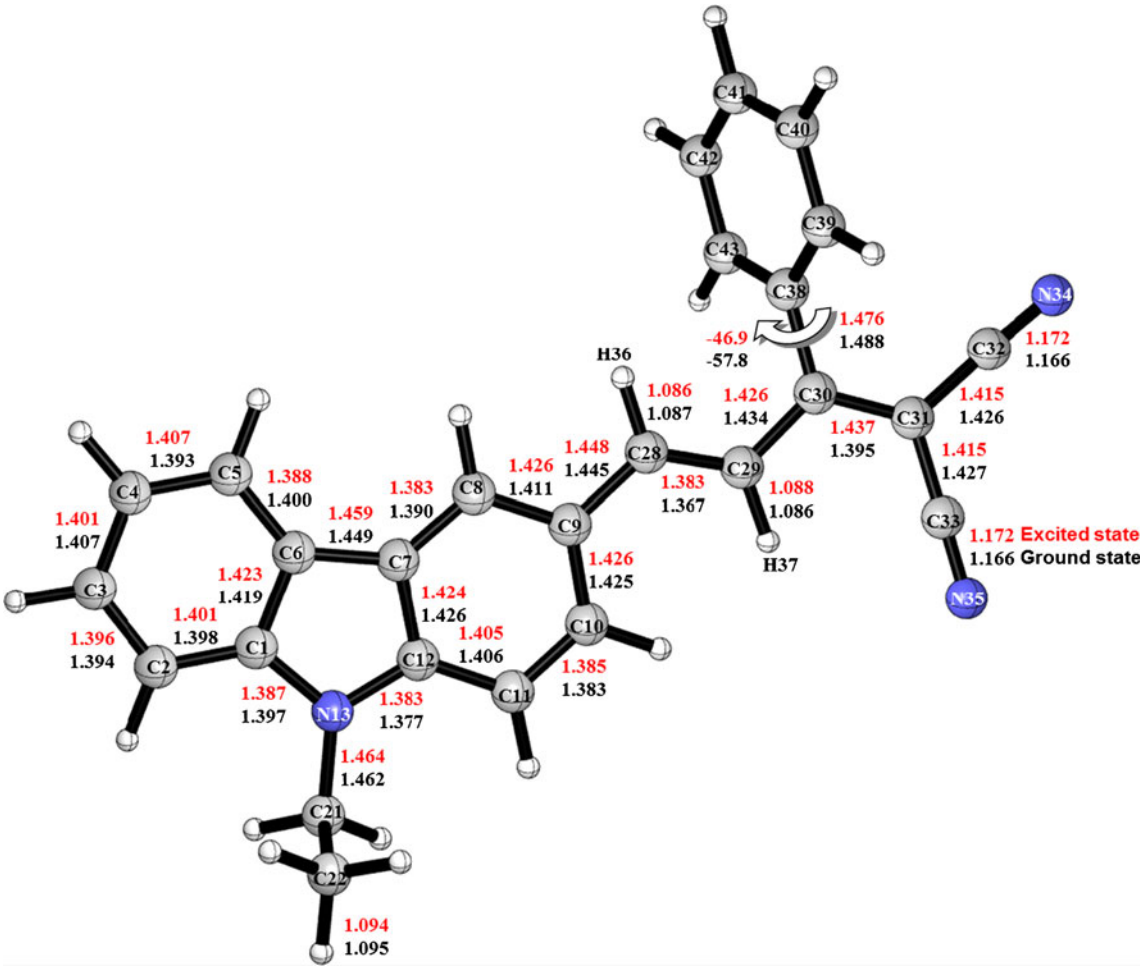

Fig. 2 Optimized geometry of **5a** in DMF solvent in the ground state and excited state (bond lengths are in Å, dihedral angles are in °)

other three dyes **5a**, **5b** and **6a**. Dye **5a** showed lower unusual lower quantum yield in toluene compared to the other solvents. Dyes **5b**, **6a** and **6b** showed low quantum yields in the solvents acetone (0.0016), methanol (0.0150) and acetone (0.0094) respectively. Quantum yields of dyes **5a**, **5b**, **6a** and **6b** were found to be comparatively higher in acetonitrile (0.0074), DCM (0.0094), toluene (0.0406) and toluene (0.0937) respectively. Push-pull charge transfer in

Table 1 Mulliken charge (e) distribution for dyes **5a**, **5b**, **6a** and **6b** in DMF in ground and excited state optimized geometry

Atom number	**5a**		**5b**		**6a**		**6b**	
	GS[a]	ES[b]	GS	ES	GS	ES	GS	ES
N_{13}	−0.619	−0.619	−0.619	−0.619	−0.612	−0.623	−0.623	−0.623
C_9	0.148	0.138	0.149	0.139	0.148	0.142	0.150	0.144
C_{28}	−0.167	−0.162	−0.171	−0.170	−0.165	−0.165	−0.171	−0.172
C_{29}	−0.209	−0.220	−0.203	−0.205	−0.205	−0.213	−0.188	−0.194
C_{30}	0.165	0.179	0.104	0.127	0.166	0.172	0.101	0.111
C_{31}	0.023	−0.000	−0.043	−0.069	0.028	0.020	−0.038	−0.050
C_{32}	0.287	0.287	0.261	0.260	0.290	0.287	0.290	0.269
C_{33}	0.301	0.296	0.664	0.654	0.304	0.300	0.644	0.641
N_{34}	−0.540	−0.549	−0.558	−0.567	−0.537	−0.542	−0.553	−0.558
N_{35}/O_{35}	−0.544	−0.551	−0.533	−0.546	−0.541	−0.546	−0.531	−0.539
H_{36}	0.174	0.178	0.168	0.173	0.177	0.179	0.171	0.174
H_{37}	0.168	0.166	0.188	0.182	0.170	0.169	0.182	0.182

[a]*GS* Ground state

[b]*ES* Excited state

Table 2 Photo-physical properties of the dyes **5a** and **5b** in different solvents

Dye	Solvents	λ_{abs}^{max} [a] (nm)	λ_{ems}^{max} [b] (nm)	λ_{exct}^{max} [c] (nm)	Stokes shift (nm)	Φ_f [d]
5a	Toluene	453	530	451	77	0.0006
	1,4-Dioxane	444	534	446	90	0.0024
	Ethyl acetate	447	548	449	101	0.0020
	DCM[e]	456	552	451	96	0.0046
	Acetone	450	558	450	108	0.0048
	Methanol	453	572	450	119	0.0082
	Acetonitrile	450	570	450	120	0.0084
	DMF[f]	457	574	452	117	0.0074
5b	Toluene	429	522	436	93	0.0039
	1,4-Dioxane	426	528	435	102	0.0056
	Ethyl acetate	426	534	447	108	0.0031
	DCM	429	547	438	118	0.0094
	Acetone	429	548	435	119	0.0016
	Methanol	429	560	440	131	0.0065
	Acetonitrile	429	560	432	131	0.0044
	DMF	430	560	436	130	0.0075

[a]Absorption wavelength maxima
[b]Fluorescence emission maxima
[c]Fluorescence excitation maxima
[d]Fluorescence quantum yield
[e]*DCM* Dichloromethane
[f]*DMF N,N*-Dimethylformamide

D-π-A and A-π-D-π-A type chromophore is shown in Fig. 4.

Our observation suggests that substantial solvent and/or intramolecular solute relaxation takes place in the more polar solvent in the excited state, stabilizing the geometry with higher charge transfer character in the excited state. This leads to the dipolar structure of the donor-acceptor based dyes Fig. 4. The rapid non-radiative relaxation of the solvent environment results in the formation of the emissive state. However, it can be noted that the predominant pathway for decay of intramolecular charge transfer in these dyes is via non-radiative decay which is indicated by the low fluorescence quantum yields (Tables 2 and 3).

Electronic Vertical Excitation Spectra

The computed vertical excitation spectra associated with their oscillator strengths, composition, and assignments of the chromophores as well as the corresponding experimental absorption wavelengths of the dyes **5a**, **5b**, **6a** and **6b** are shown in Tables 4, 5, 6 and 7. As mentioned earlier in "Solvatochromism and Solvatofluorism", for dye **5b** the absorption maxima remained fairly constant in all solvents while their fluorescence maxima increased progressively with the increase in the solvent polarity resulting in the increased Stokes shift with the increase in the solvent polarity. In case of dyes **5a**, **6a** and **6b**, both the absorption

Table 3 Photo-physical properties of the dyes **6a** and **6b** in different solvents

Dye	Solvents	λ_{abs}^{max} (nm)	λ_{ems}^{max} (nm)	λ_{exct}^{max} (nm)	Stokes shift (nm)	Φ_f
6a	Toluene	474	526	478	52	0.0406
	1,4-Dioxane	465	536	473	71	0.0382
	Ethyl acetate	468	550	477	82	0.0320
	DCM	477	553	484	76	0.0375
	Acetone	474	568	479	94	0.0382
	Methanol	474	578	481	104	0.0150
	Acetonitrile	471	578	479	107	0.0299
	DMF[e]	484	584	486	100	0.0366
6b	Toluene	450	524	453	74	0.0937
	1,4-Dioxane	447	530	450	83	0.0881
	Ethyl acetate	448	546	454	98	0.0154
	DCM	457	554	460	97	0.0145
	Acetone	451	552	455	101	0.0094
	Methanol	457	570	460	113	0.0522
	Acetonitrile	450	572	457	122	0.0500
	DMF	457	574	461	115	0.0840

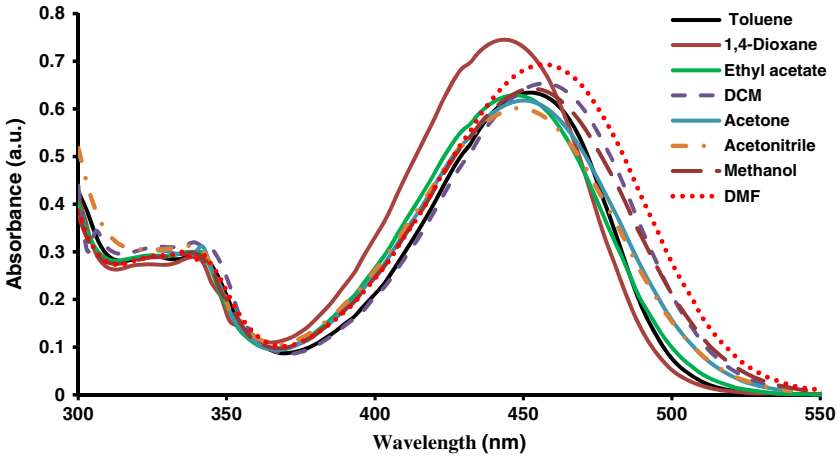

Fig. 3 Absorption spectra of dye **5a** in different solvents
Note: a.u. = arbitrary unit

maxima and Stokes shift increased with the increase in the solvent polarity. This observation is in agreement with the photo-induced charge transfer or charge-separated emissive state, for which a steadily higher stabilization in increasingly polar solvents should be anticipated and leading to an increase in the Stokes shift. All the four dyes showed absorption band with one shoulder peak at the shorter wavelength. The shorter absorption band is due to the $\pi \rightarrow \pi^*$ transitions occuring at the higher energy and the longer absorption band with higher oscillator strength at lower energy is due to intramolecular charge transfer characteristic of donor-π-acceptor push-pull dyes (Tables 4, 5, 6 and 7).

The charge transfer band for all four dyes are mainly due to the electronic transition from highest occupied molecular orbital (HOMO) to lowest unoccupied molecular orbital (LUMO) whereas the other shorter electronic excitation is due to the HOMO-2 → LUMO transition for the dyes **5a** and **5b**; and HOMO → LUMO+1 for the dye **6a** whereas HOMO-1 → LUMO+1 for dye **6b**. Tables 4, 5, 6 and 7 showed a correlation between the experimentally obtained absorption wavelength maxima and TD-B3LYP/6-31G(d) computed vertical excitation for these dyes.

Dye **5a** showed the lowest experimental absorption wavelength band in 1,4-dioxane (444 nm) and highest in DMF (457 nm) solvent whereas the computed vertical excitation is found lowest in 1,4-dioxane (456 nm) and highest in DMF (473 nm). Similarly, solvatochromism results were obtained for the other three dyes **5b**, **6a** and **6b**. The largest wavelength difference between the experimental absorption maxima and computed vertical excitation is 20 nm (acetonitrile) for dye **5a**. On moving from 1,4-dioxane to DMF, 13 nm shift in the absorption band was observed for dye **5a** and 16 nm shift was observed in the computed vertical excitation spectra. The largest wavelength difference between the experimental absorption maxima and computed vertical excitation was 32 (DMF), 36 and 45 nm (acetonitrile) for dyes **5b**, **6a** and **6b**.

The experimentally obtained fluorescence emission spectral data and emission computed from TD-B3LYP/6-31G(d) computations are shown in Table 8. All the four dyes showed an increase in the emission wavelength as the solvent polarity increases. The experimental emission wavelength and emission computed by TD-B3LYP/6-31G(d) showed a largest difference of 54 nm (1,4-dioxane), 61 nm (methanol) for dyes **5a** and **5b**; and 35 nm (DMF) and 37 nm (1,4-dioxane) were obtained for dyes **6a** and **6b**. A good correlation has been obtained between experimentally recorded emissions against the emissions computed from TD-B3LYP/6-31G(d) for the synthesized dyes in the different solvents (Figs. 5, S11–S13). These dyes showed a small Stokes shift in 1,4-dioxane whereas large Stokes shift was observed in DMF solvent. Such changes in the Stokes shift are due to the lowering of HOMO and LUMO orbital band gap.

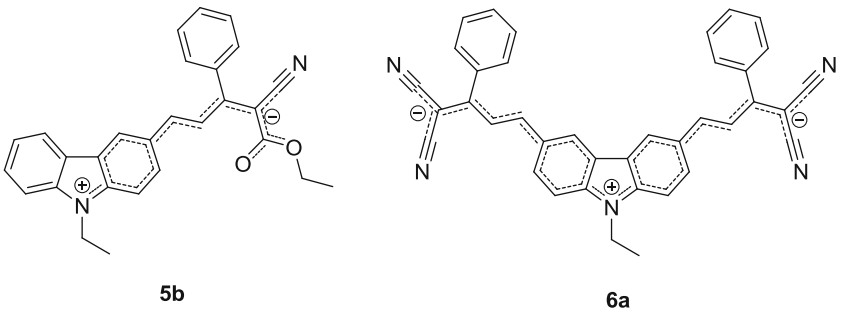

Fig. 4 Dipolar structures of the dyes **5b** and **6a**

Table 4 Observed UV-visible absorption and computed vertical excitation spectra of dye **5a** in different solvents

Solvent	Exp.[a]	TD-B3LYP/6-31G(d)[b]		
	λ_{abs}^{max} (nm)	Vertical excitation (nm)	Oscillator strength *f*	Major contribution[c]
1,4-Dioxane	444	456	1.0642	H[d] → L[e] (0.6988)
	339	340	0.2643	H-2 → L (0.6245)
Toluene	453	459	1.0894	H → L (0.6999)
	339	341	0.2670	H-2 → L (0.6281)
Ethyl acetate	447	465	1.0302	H → L (0.6977)
	339	343	0.2865	H-2 → L (0.6300)
DCM	456	469	1.0497	H → L (0.6987)
	339	344	0.2923	H-2 → L (0.6352)
Acetone	450	470	1.0188	H → L (0.6972)
	342	344	0.2993	H-2 → L (0.6361)
Methanol	453	469	1.0038	H → L (0.6964)
	339	344	0.3014	H-2 → L (0.6359)
Acetonitrile	450	470	1.0111	H → L (0.6968)
	339	344	0.3018	H-2 → L (0.6369)
DMF	457	473	1.0491	H → L (0.6987)
	342	345	0.3018	H-2 → L (0.6409)

[a]Experimental absorption wavelength, λ_{abs}^{max}

[b]TD-B3LYP/6-31G(d) computations

[c]Electronic transition (CI expansion coefficient for given excitation)

[d]*H* HOMO

[e]*L* LUMO

Frontier Molecular Orbitals (FMOs)

The effect of the donor-acceptor properties of two different groups with carbazole ring was studied by examining the different HOMO and LUMO levels of the synthesized dyes. The relative ordering of the occupied and virtual orbitals provides a reasonable qualitative indication of the excitation properties and the ability of hole or electron injection. The first dipole-allowed electronic transitions, and the strongest electron transitions with largest oscillator strength, usually correspond almost exclusively to the promotion of an electron from HOMO → LUMO. Figure 6 displayed the energies of the different molecular orbitals involved in the electronic transitions of the representative two classes of dyes (**5b** and **6a**) in different solvents. It is observed that the electron transition in each

Table 5 Observed UV-visible absorption and computed vertical excitation spectra of dye **5b** in different solvents

Solvent	Exp.	TD-B3LYP/6-31G(d)		
	λ_{abs}^{max} (nm)	Vertical excitation (nm)	Oscillator strength *f*	Major contribution
1,4-Dioxane	426	446	1.1578	H → L (0.7015)
	333	339	0.1694	H-2 → L (0.5605)
Toluene	429	449	1.1802	H → L (0.7022)
	336	341	0.2670	H-2 → L (0.6546)
Ethyl acetate	426	454	1.1195	H → L (0.7009)
	333	343	0.1930	H-2 → L (0.5613)
DCM	429	458	1.1352	H → L (0.7015)
	336	341	0.2025	H-2 → L (0.5687)
Acetone	429	459	1.1049	H → L (0.7006)
	327	341	0.2106	H-2 → L (0.5691)
Methanol	429	459	1.0904	H → L (0.7001)
	336	341	0.2129	H-2 → L (0.5686)
Acetonitrile	429	459	1.0907	H → L (0.7004)
	333	341	0.2142	H-2 → L (0.5704)
DMF	430	462	1.1312	H → L (0.7015)
	336	341	0.2177	H-2 → L (0.5777)

Table 6 Observed UV-visible absorption and computed vertical excitation spectra of dye **6a** in different solvents

Solvent	Exp.	TD-B3LYP/6-31G(d)		
	λ_{abs}^{max} (nm)	Vertical excitation (nm)	Oscillator strength *f*	Major contribution
1,4-Dioxane	465	488	1.4753	H → L (0.7030)
	414	437	0.0472	H → L+1 (0.6091)
Toluene	474	491	1.5091	H → L (0.7029)
	411	438	0.0527	H → L+1 (0.6152)
Ethyl acetate	468	499	1.4535	H → L (0.7034)
	414	445	0.0433	H → L+1 (0.6006)
DCM	477	504	1.4805	H → L (0.7034)
	423	447	0.0468	H → L+1 (0.6040)
Acetone	474	506	1.4501	H → L (0.7036)
	420	450	0.0416	H → L+1 (0.5963)
Methanol	474	506	1.4347	H → L (0.7037)
	417	450	0.0394	H → L+1 (0.5929)
Acetonitrile	471	507	1.4432	H → L (0.7036)
	417	451	0.0405	H → L+1 (0.5943)
DMF	484	509	1.4864	H → L (0.7036)
	423	451	0.0467	H → L+1 (0.6021)

case included a HOMO → LUMO transition (Figs. 6 and 7 and Tables 4, 5, 6 and 7).

In the case of mono-styryl D-π-A dye **5b**, the energies of the HOMO and LUMO orbitals were lowered as the solvent polarity was increased. But the extent of decrease in energy level was found to be more in the case of the LUMO (0.148 eV) as compare to HOMO (0.048 eV). This suggests that the LUMO orbital is more relaxed in the polar solvent (Fig. 6 and Tables S1–S2). Another electronic transition in dye **5b** appeared as a small band due to HOMO-2 → LUMO transition (Table 5 and Fig. 7).

But, in case of the bis-styryl A-π-D-π-A dye **6a**, the energy of the LUMO orbitals (0.037 eV) were lowered less than the HOMO (0.136 eV) which is due to the stabilization

Table 7 Observed UV-visible absorption and computed vertical excitation spectra of dye **6b** in different solvents

Solvent	Exp.	TD-B3LYP/6-31G(d)		
	λ_{abs}^{max} (nm)	Vertical excitation (nm)	Oscillator strength *f*	Major contribution
1,4-Dioxane	447	474	1.5292	H → L (0.7029)
	399	384	0.5505	H-1 → L+1 (0.6878)
Toluene	450	477	1.5602	H → L (0.7028)
	402	385	0.5231	H-1 → L+1 (0.6883)
Ethyl acetate	448	486	1.4982	H → L (0.7034)
	402	392	0.5202	H-1 → L+1 (0.6895)
DCM	457	491	1.5230	H → L (0.7034)
	402	394	0.5114	H-1 → L+1 (0.6902)
Acetone	451	494	1.4945	H → L (0.7037)
	402	396	0.5099	H-1 → L+1 (0.6906)
Methanol	457	494	1.4804	H → L (0.7038)
	402	397	0.5107	H-1 → L+1 (0.6907)
Acetonitrile	450	495	1.4886	H → L (0.7038)
	402	397	0.5095	H-1 → L+1 (0.6908)
DMF	459	497	1.5300	H → L (0.7036)
	402	398	0.5041	H-1 → L+1 (0.6911)

Table 8 Experimental UV-visible emission and computed emission from TD-B3LYP/6-31G(d) computations for dyes **5a** and **5b** in different solvents

Solvents	**5a**		**5b**		**6a**		**6b**	
	Exp.[a] λ_{ems}^{max} (nm)	TD-B3LYP/ 6-31G(d) emission (nm)[b]	Exp. λ_{ems}^{max} (nm)	TD-B3LYP/ 6-31G(d) emission (nm)	Exp. λ_{ems}^{max} (nm)	TD-B3LYP/ 6-31G(d) emission (nm)	Exp. λ_{ems}^{max} (nm)	TD-B3LYP/ 6-31G(d) emission (nm)
1,4-Dioxane	534	480	522	465	526	504	530	493
Toluene	530	482	528	467	536	507	524	495
Ethyl acetate	548	503	534	492	550	531	546	519
Methanol	572	521	560	499	578	549	570	538
Acetone	558	518	548	508	568	546	552	535
Acetonitrile	570	522	560	511	578	549	572	538
DCM	552	510	547	511	553	538	554	526
DMF	574	522	560	511	584	549	574	539

[a] Experimentally recorded emission maxima

[b] Emission computed using TD-B3LYP/6-31G(d) level

of the HOMO orbital in dye **6a** in more polar solvents. Also, the energy of LUMO+1 orbital in dye **5b** is largely separated from LUMO whereas in dye **6a** the energy of LUMO+1 orbital is closely situated near to LUMO orbital. Due to the lowering of energy of LUMO+1, the dye **6a** showed another absorption band at the higher wavelength as a shoulder peak (Table 6 and Figure S15) arising from HOMO → LUMO+1 transition which was observed in mono-styryl dye **5b** (Table 5 and Figure S14). Such transitions were also observed for the other two dyes **5a** and **6b**.

To understand the above electronic transitions in the perspective of the orbital picture, the molecular HOMOs and LUMOs were generated by using GaussView 5.0 software [55]. The HOMO and LUMO plots are given in the Figs. 8 and 9 for dyes **5a**, **5b**, **6a** and **6b**. As expected, HOMO and LUMO are π-orbitals. It has been observed that the HOMO and LUMO of the dyes are fully delocalized on the donor carbazole ring, phenyl ring and acceptor cyano or carbethoxy group through the π-bond conjugation.

Moreover, the electron densities in the HOMOs of dyes **5b** and **6a** are largely located on the *N*-ethyl carbazole on the donor and the electron densities in the LUMO of dyes **5b** and **6a** are heavily located toward the acceptor through π-bridge. These excitations mostly consist of the charge transfer from the *N*-ethyl carbazole on the donor to the acceptor end. The energy gap of HOMO → LUMO explains the charge transfer interactions within the dye, which also influences the first hyperpolarizability of the dyes. Dye **5a** showed longer wavelength absorption is due to the transition from HOMO → LUMO and the shorter absorption band is due to the HOMO-2 → LUMO transition (Figure S14). But, in case of dyes **6a** and **6b** (Figures S15–S16) it is clear that they have a longer wavelength absorption is due to HOMO →

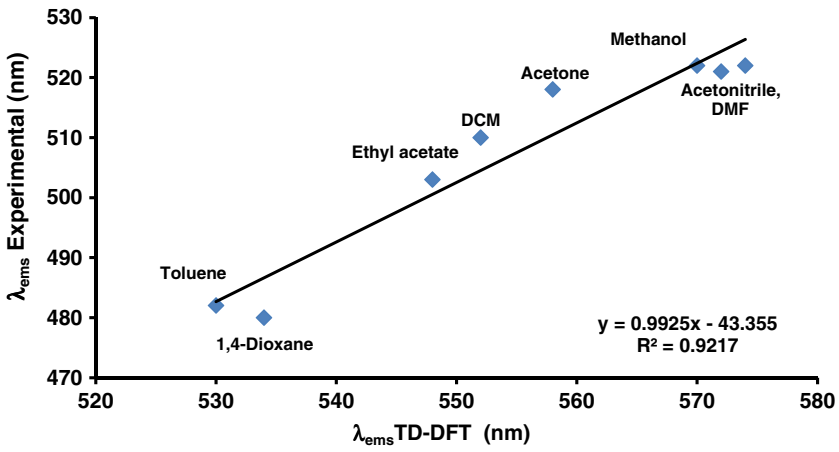

Fig. 5 Plot of experimental emission maxima versus emission calculated from excited state optimization for dye **5a**

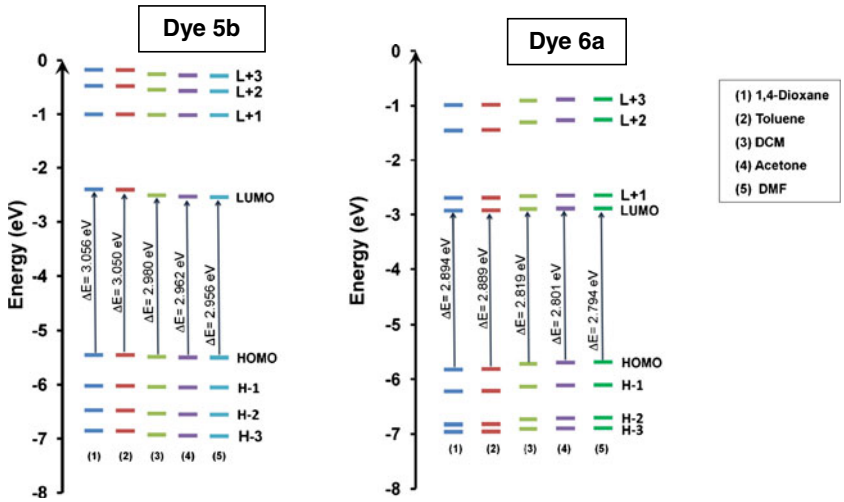

Fig. 6 FMO energy level diagram of dyes **5b** and **6a**

LUMO transition and the shoulder peak is due to transition occurring from HOMO → LUMO+1 (dye **6a**) and HOMO-1 → LUMO+1 (dye **6b**).

Dipole Moment Determination

It is well known that the dipole moment of D-π-A-like molecules is determined by the donor-acceptor strength. The ground and excited state geometries of an organic compound decide its electronic spectral behaviour. When such a molecule is placed in a solvent environment, the spectral behaviour is influenced by the properties of the solvent like dielectric constant, polarity and viscosity. This affects the absorption and emission spectra of the molecule. In other words, the effect of solvent on the absorption and emission spectra clearly indicates the change in the dipolar characteristics of the molecule in the excited state. Solvatochromism and solvatofluorism are effective tools to understand the change in the dipole moment of the molecule experiencing at the first singlet excited state. The solvent dependence of absorption and fluorescence maxima were used to estimate the excited state dipole moment [56–68]. This technique is based on a linear relation between the absorption, emission maxima and polarity functions of a solvent [69] which is dependent on both the relative permittivity (ε) and refractive index (η) of the solvent medium. Among the techniques available for the determination of the excited state dipole moments, the most popular is that based on Lippert-Mataga equation [34–39].

In this paper, we report the ground and excited state dipole moments of dyes **5a**, **5b**, **6a** and **6b** by solvatochromic method using Bakhshiev [40] and Kawski-Chamma-Viallet correlations [41–43]. It must be noted here that the Lippert-Mataga

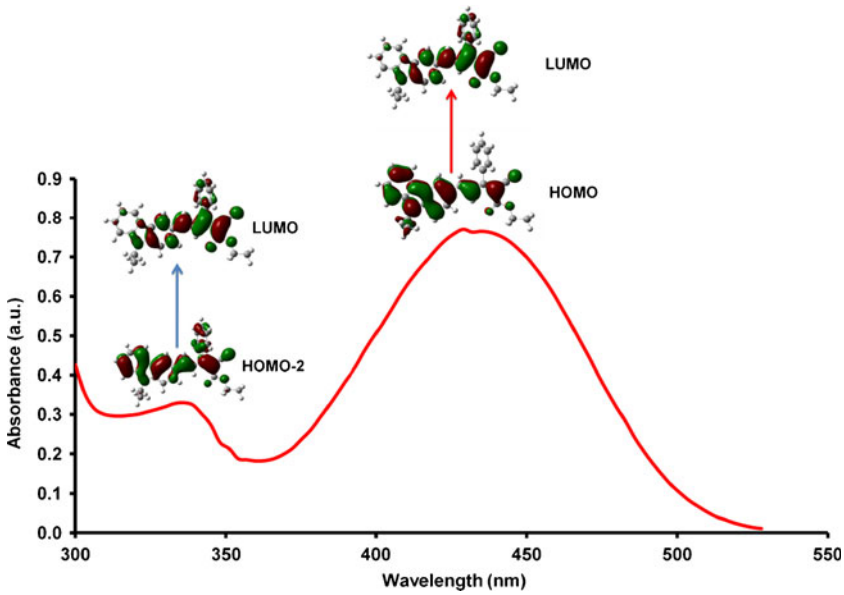

Fig. 7 Electronic transitions for dye **5b**
Note: a.u. = arbitrary unit

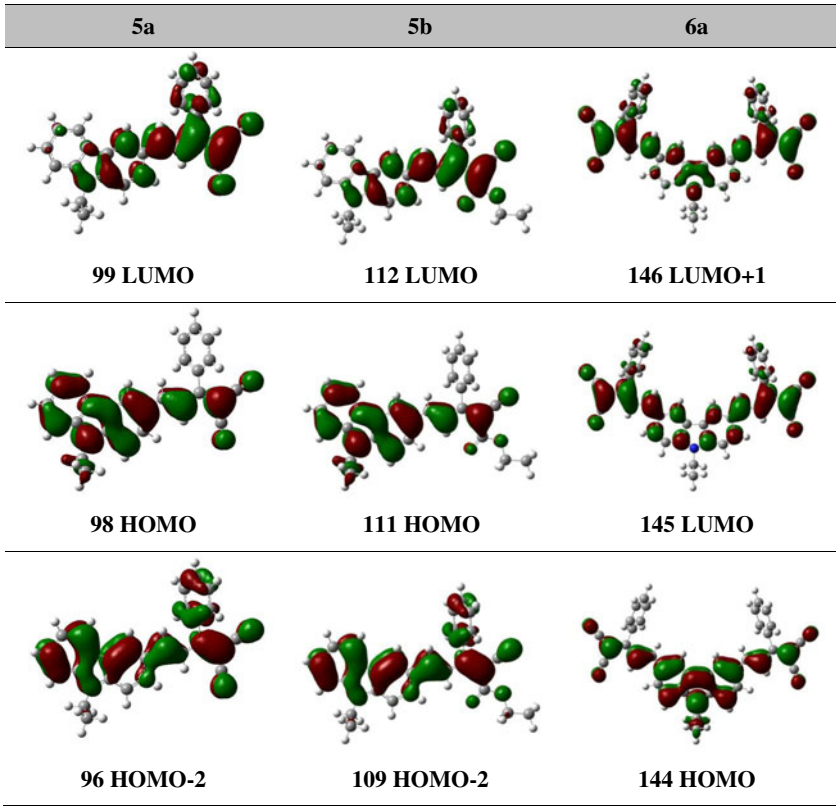

Fig. 8 Frontier molecular orbitals of dyes **5a**, **5b** and **6a**

correlation does not account for the hydrogen bonding effects and formation of molecular complexes.

Theory and Calculations

Equations 1–11 were used to determine the ground and excited singlet state dipole moments by the solvatochromic method.

Lippert's Formula

$$\overline{\nu}_a - \overline{\nu}_f = \mathrm{m} f(\varepsilon,\eta) + \text{Constant} \tag{1}$$

here, $\overline{\nu}_a$ and $\overline{\nu}_f$ are the wavelengths of the absorption and emission maxima in wave number (cm^{-1}) respectively. $f(\varepsilon,\eta)$ is Lippert's polarity function and m is the slope of the graph obtained by plotting $f(\varepsilon,\eta)$ versus Stokes shift ($\overline{\nu}_a - \overline{\nu}_f$).

Bakhshiev's Formula

$$\overline{\nu}_a - \overline{\nu}_f = m_1 f_1(\varepsilon,\eta) + \text{Constant} \tag{2}$$

$f_1(\varepsilon,\eta)$ is Bakhshiev's polarity function and m_1 is the slope of the graph obtained by plotting $f_1(\varepsilon,\eta)$ versus Stokes shift ($\overline{\nu}_a - \overline{\nu}_f$) as shown in Fig. 10.

$f_1(\varepsilon,\eta)$ and m_1 are defined as follows:

$$f_1(\varepsilon,\eta) = \frac{2\eta^2+1}{\eta^2+2}\left[\frac{\varepsilon-1}{\varepsilon+2} - \frac{\eta^2-1}{\eta^2+2}\right] \tag{3}$$

$$m_1 = \frac{2\left(\mu_e - \mu_g\right)^2}{hca_0^3} \tag{4}$$

here, h is Planck's constant, c is the velocity of light in vacuum, μ_g is the dipole moment in the ground state, μ_e is the dipole moment in the excited singlet state, a_0 is the Onsager cavity radius, ε is the solvent dielectric constant and η is the solvent refractive index.

Kawski–Chamma–Viallet's Formula

$$\frac{\overline{\nu}_a + \overline{\nu}_f}{2} = -m_2 f_2(\varepsilon,\eta) + \text{Constant} \tag{5}$$

Here the meaning of the symbols is the same as in Eqs. (1) and (2), except for $f_2(\varepsilon,\eta)$ and m_2 which are defined as follows:

$$f_2(\varepsilon,\eta) = \frac{2\eta^2+1}{2(\eta^2+2)}\left[\frac{\varepsilon-1}{\varepsilon+2} - \frac{\eta^2-1}{\eta^2+2}\right] + \frac{3}{2}\left[\frac{\eta^4-1}{(\eta^2+2)^2}\right] \tag{6}$$

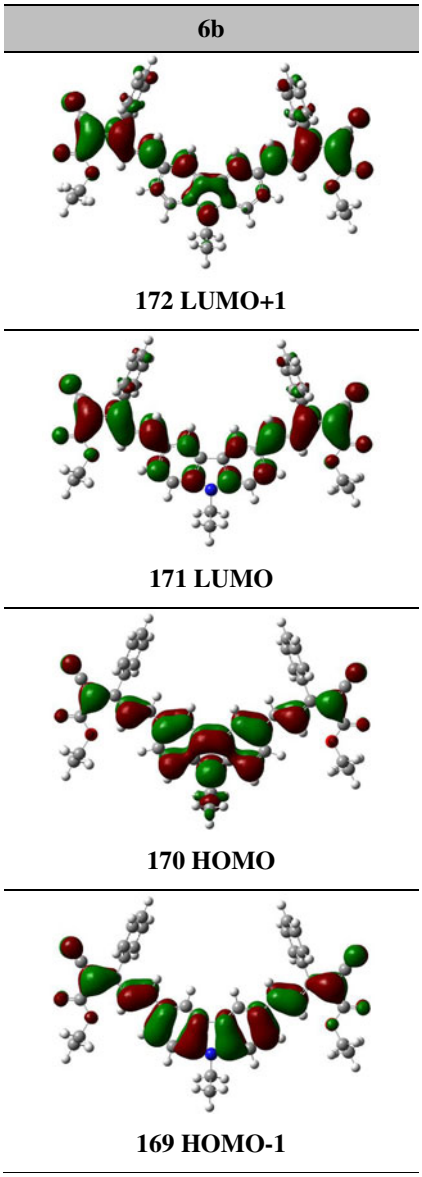

Fig. 9 Frontier molecular orbitals of dye **6b**

and

$$m_2 = \frac{2\left(\mu_e^2 - \mu_g^2\right)}{hca_0^3} \tag{7}$$

The values for refractive index and dielectric constant were substituted in the Eqs. (3) and (6) and the solvent polarity functions f_1 (ε, η) and f_2 (ε, η) were calculated and tabulated in the Table 9. The parameters m_1 and m_2 can be obtained from the absorption and emission band shifts Eqs. (2) and (5) (Figs. 10 and 11). Basically m_1 and m_2 are the slopes which can be calculated using Eqs. (2) and (5) respectively.

Assuming the ground and excited state dipole moments to be parallel, the following expressions are obtained on the basis of Eqs. (4) and (7) [42, 43];

$$\mu_e = \frac{|m_1 + m_2|}{2}\left(\frac{hca_0^3}{2m_1}\right)^{1/2} \tag{8}$$

$$\mu_g = \frac{|m_2 - m_1|}{2}\left(\frac{hca_0^3}{2m_1}\right)^{1/2} \tag{9}$$

The value of the Onsager cavity radius (a_0) is usually calculated from molecular volume according to Suppan's equation [70] as shown in Eq. (10).

$$a_0 = \left(\frac{3M}{4\pi\delta N}\right)^{1/3} \tag{10}$$

Where δ is the density of solute molecule, M the molecular weight of the solute and N is the Avogadro's number. The value of (a_0) can also be conveniently computed from the optimized ground state geometry of molecule [66, 71–75].

In this paper, we used the Onsager radii obtained from the optimized ground state in different solvents at B3LYP/6-31G(d) level of theory using PCM model. Usually an assumption is made that the Onsager radii does not deviate much at the excited state from the ground state. Therefore, a ratio of excited state dipole moment to the ground state dipole moment can be obtained by dividing Eq. (8) by Eq. (9). With the assumption that (a_0) is same in ground and excited state, the ratio μ_e/μ_g is given by Eq. (11).

$$\frac{\mu_e}{\mu_g} = \frac{|m_1 + m_2|}{|m_1 - m_2|}; \quad (m_2 > m_1) \tag{11}$$

However, when the optimized excited state geometry was used to compute Onsager radii at the same level of theory, it was found that they are not same. The Onsager radii values obtained from B3LYP/6-31G(d) and TD-B3LYP/6-31G(d) for the ground and excited states in different solvents are summarized in Table S3. Therefore, the ground and excited state dipole moments were individually obtained from Eqs. (8) and (9) using (a_0) for ground and excited state respectively and the experimental solvatochromic and solvatofluoric data and summarized in Table 10. The dipole moments obtained from solvatochromic method showed that the excited state of dyes **5a**, **5b**, **6a** and **6b** are having higher dipole moment values than in ground state which in fact accounts for the prominent charge transfer processes occurring in the excited state.

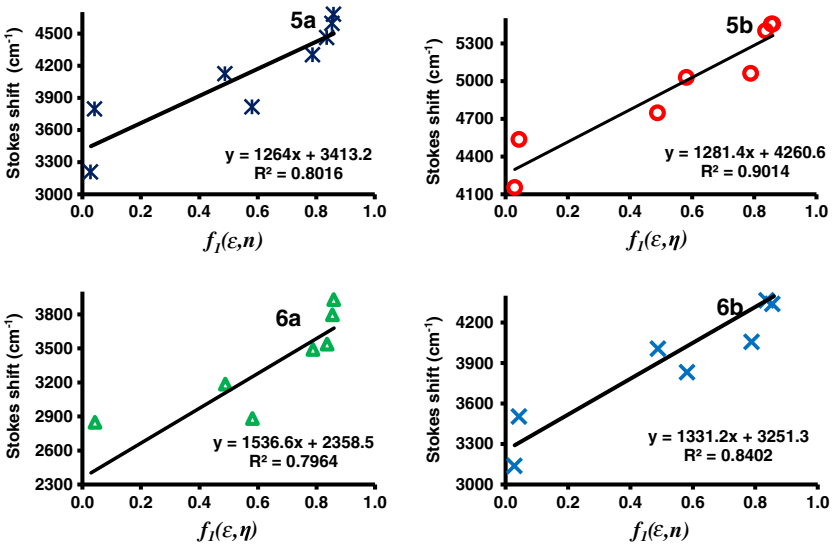

Fig. 10 Plot of Stokes shift (Δv) with solvent polarity parameter $f_1(\varepsilon,\eta)$ for dyes **5a**, **5b**, **6a** and **6b**

Static Second-Order Nonlinear Optical (NLO) Properties

Organic nonlinear optical (NLO) materials are presently attracting significant attention because of their advantages over the inorganic materials. The donor-π-acceptor molecules have been successfully used in the development of the second-order organic NLO materials. The first hyperpolarizability (β_o) value can be enhanced by design of planar D-π-A molecule, the bond length alternation theory, and their relative orientations lead to substantial increases in β_o values. The large first hyperpolarizability responses have been observed by using polyene as π-conjugated bridges to the donor-acceptor groups attached to a heterocyclic ring [76, 77]. Thus, push-pull heterocyclic chromophores have attracted considerable interest due to their good linear and nonlinear optical properties. It is well-known that the charge transfer from a donor to an acceptor across a π-electron bridge would interrupt the aromaticity of the π-conjugation bridge and this leads to substantial decrease of the aromatic delocalization energy by the means of introduction of a heterocyclic ring. This would facilitate the charge-transfer state to dominate the exited state and enhance the second-order NLO responses.

Here, second-order NLO properties of the carbazole-cored D-π-A and A-π-D-π-A chromophores were calculated by using density functional theory (DFT). The static first hyperpolarizability (β_o) and its related properties for dyes **5a**, **5b**, **6a** and **6b** calculated using B3LYP/6-31G(d) on the basis of the finite field approach. In the presence of an applied field, the energy of the system is a function of the electric field, and the first hyperpolarizability is a third rank tensor that can be described by a 3×3×3 matrix. The 27 components of the 3D matrix can be reduced to 10 components because of the Kleinman symmetry [78]. The matrix can be given in the lower tetrahedral format. It is obvious that the lower part of the 3×3×3 matrix is a tetrahedral. The components of β are defined as the co-efficient in the Taylor series expansion of the energy in the external electric field. When the external electric field is weak and homogeneous, this expansion becomes.

$$E = E^{\circ} - \mu_\alpha F_\alpha - 1/2\alpha_{\alpha\beta} F_\alpha F_\beta - 1/6\beta_{\alpha\beta\gamma} F_\alpha F_\beta F_\gamma + \cdots \quad (12)$$

Where E° is the energy of the unperturbed molecules, F_α is the field at the origin, μ_α, $\alpha_{\alpha\beta}$ and $\beta_{\alpha\beta\gamma}$ are the components of dipole moment, polarizability and the first hyperpolarizabilities, respectively.

The total static dipole moment μ, the mean polarizability α_0, the anisotropy of the polarizability $\Delta\alpha$ and the mean first hyperpolarizability β_o, using the x-, y- and z-components are defined as

$$\beta = \left(\beta_x^2 + \beta_y^2 + \beta_z^2\right)^{1/2} \quad (13)$$

$$\alpha_0 = \frac{\alpha_{xx} + \alpha_{yy} + \alpha_{zz}}{3} \quad (14)$$

$$\Delta\alpha = 2^{-1/2}\left[\left(\alpha_{xx} + \alpha_{yy}\right)^2 + \left(\alpha_{zz} + \alpha_{xx}\right)^2 + 6\alpha_{xx}^2\right]^{1/2} \quad (15)$$

$$\beta_o = \left(\beta_x^2 + \beta_y^2 + \beta_z^2\right)^{1/2} \quad (16)$$

The value of second order-optical susceptibility $\chi^{(2)}$ in a given NLO system depends on the molecular hyperpolarizability, β_o, the number of chromophores and the degree of non-centrosymmetry. The computed first

Table 9 Solvatochromism data and solvent polarity parameters of dyes **5a**, **5b**, **6a** and **6b** with the calculated values of $f_1(\varepsilon,\eta)$ and $f_2(\varepsilon,\eta)$

Solvent	Dye	$\bar{\nu}_a$ [a] (cm^{-1})	$\bar{\nu}_f$ [b] (cm^{-1})	$\Delta\bar{\nu}$ [c] (cm^{-1})	$\frac{(\bar{\nu}_a+\bar{\nu}_f)}{2}$	ε [d]	η [e]	E_N^{Tf}	$f_1(\varepsilon,\eta)$ [g]	$f_2(\varepsilon,\eta)$ [h]
Toluene	**5a**	22075	18868	3207	20471	2.38	1.497	0.099	0.0290	0.3499
	5b	23310	19157	4153	21234					
	6a	21097	19011	2086	20054					
	6b	22222	19084	3138	20653					
1,4-Dioxane	**5a**	22523	18727	3796	20625	2.21	1.420	0.164	0.0430	0.3066
	5b	23474	18939	4535	21207					
	6a	21505	18657	2849	20081					
	6b	22371	18868	3503	20620					
Ethyl acetate	**5a**	22371	18248	4123	20310	6.02	1.372	0.228	0.4891	0.4979
	5b	23474	18727	4748	21100					
	6a	21368	18182	3186	19775					
	6b	22321	18315	4006	20318					
Methanol	**5a**	22075	17483	4593	19779	32.70	1.326	0.775	0.8554	0.6498
	5b	23310	17857	5453	20584					
	6a	21097	17301	3796	19199					
	6b	21882	17544	4338	19713					
Acetone	**5a**	22222	17921	4301	20072	20.70	1.364	0.335	0.7887	0.6421
	5b	23310	18248	5062	20779					
	6a	21097	17606	3491	19351					
	6b	22173	18116	4057	20144					
Acetonitrile	**5a**	22222	17544	4678	19883	35.94	1.342	0.460	0.8599	0.6629
	5b	23310	17857	5453	20584					
	6a	21231	17301	3930	19266					
	6b	22222	17483	4740	19852					
DCM	**5a**	21930	18116	3814	20023	8.93	1.445	0.309	0.5816	0.5924
	5b	23310	18282	5028	20796					
	6a	20964	18083	2881	19524					
	6b	21882	18051	3831	19966					
DMF	**5a**	21882	17422	4460	19652	36.71	1.427	0.386	0.8367	0.7081
	5b	23256	17857	5399	20556					
	6a	20661	17123	3538	18892					
	6b	21786	17422	4365	19604					

[a] Absorption maxima in wavenumber

[b] Fluorescence maxima in wavenumber

[c] Stokes shift

[d] Dielectric constant

[e] Refractive index

[f] E_N^T values were taken from ref. [70]

[g and h] Polarity functions

hyperpolarizability, β_o, of dyes was found to be ranging from 124.44×10^{-30} (dye **5a**), 120.52×10^{-30} (dye **5b**), 119.21×10^{-30} (dye **6a**) and 96.54×10^{-30} (dye **6b**) e.s.u. (Table S4). These values are greater than urea (0.38×10^{-30} e.s.u.) by 327, 390, 313 and 253 times. As expected, these dyes have shown a large hyperpolarizability suggesting considerable charge transfer characteristics of the first excited state which is further supported by the large difference in the dipole moments between the ground and excited states from the solvatochromism studies. These dyes can

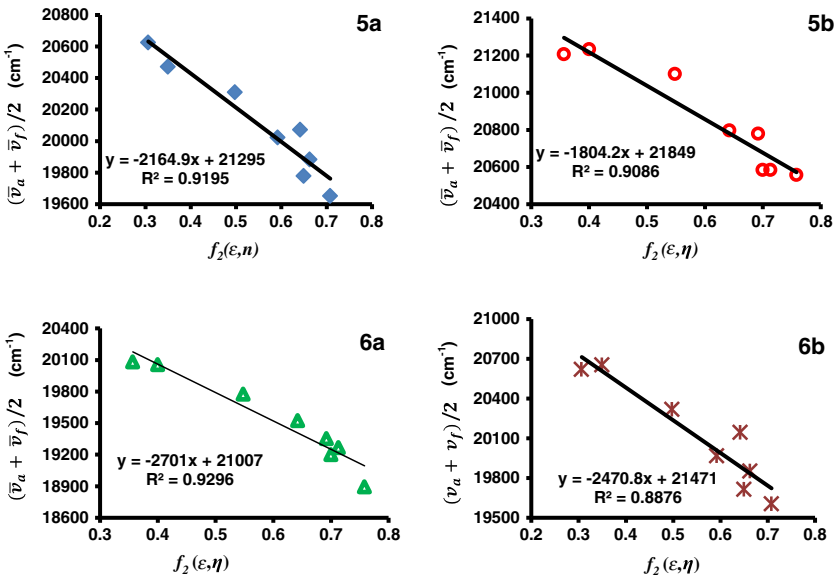

Fig. 11 Plot of $(\bar{\nu}_a + \bar{\nu}_f)/2$ with solvent polarity parameter $f_2(\varepsilon,\eta)$ for dyes **5a**, **5b**, **6a** and **6b**

be used as a promising candidate in the field of non-linear optics.

Conclusions

In this paper, we have studied properties and electronic spectral behaviour of four dyes in solvents of varying polarities. The solvatochromism data shows these dyes have a larger Stokes shift which increases with the solvent polarity. Solvatochromism studies showed that there is a large increase in the dipole moment of the first excited state suggesting a pronounced change delocalization in the first excited state. The optimized geometries obtained from B3LYP/6-31G(d) and TD-B3LYP/6-31G(d) were examined by comparing ground and excited state geometries and charge distribution. Vertical excitations and emissions were computed and compared with the experimental values. These dyes have shown a prominent absorption at the longer wavelength due to HOMO → LUMO transition with high oscillator strength and a small oscillator strength absorption band due to HOMO-2 → LUMO for dyes **5a** and **5b** whereas HOMO → LUMO+1 and HOMO-1 → LUMO+1 correspond to dyes **6a** and **6b** respectively. The computed absorption and emission wavelengths are in good agreement with the experimental results. The first hyperpolarizability was calculated using finite field approach and found that these dyes possess a large second-order nonlinear property and this is mainly due to the strong donor-π-acceptor conjugation which is attributed to the excited state intramolecular charge transfer. In summary this paper describes the importance of DFT (B3LYP) in understanding the

Table 10 Calculated dipole moments (in Debye) of dyes **5a**, **5b**, **6a** and **6b** in ground and excited state in different solvents using solvatochromism method

Solvent	ε	**5a**		**5b**		**6a**		**6b**	
		μ_g	μ_e	μ_g	μ_e	μ_g	μ_e	μ_g	μ_e
1,4-Dioxane	2.21	0.99	5.97	1.08	6.39	2.40	9.46	2.60	11.02
Toluene	2.38	1.06	6.25	1.03	6.05	2.59	10.71	2.61	10.09
DCM	8.93	1.03	6.60	1.08	6.46	2.44	9.60	2.81	10.53
Ethyl acetate	6.02	0.98	6.31	1.04	6.20	2.58	10.09	2.60	10.12
Acetone	20.70	0.96	6.00	1.13	6.08	2.37	9.22	2.69	10.55
Methanol	32.70	1.03	5.89	0.97	6.27	2.34	10.30	2.71	10.62
Acetonitrile	35.94	1.06	5.83	1.06	6.68	2.52	8.93	2.64	10.67
DMF	36.71	1.10	6.23	1.04	6.63	2.42	9.26	2.71	10.07

photophysical behaviour at molecular level of donor-π-acceptor push-pull chromophores in the light of experimental findings on solvatochromism and solvatofluorism.

Acknowledgments N.S. and V.G. are thankful to the 5th UGC-TEC Consortium agreement for financial support. A.T. is grateful to UGC for research support under Major Research Project as well as UGC-CSIR fellowship. V.P. is thankful for postdoctoral fellowship from the Principal Scientific Adviser (PSA), Govt of India. K.P. and P.U. are thankful to UGC-CAS for providing research fellowship under Special Assistance Programme (SAP). Facilities from University of Mauritius are acknowledged. The authors acknowledge the comments from anonymous reviewers to improve the manuscript.

References

1. Zhang W, He Z, Mu L, Zou Y, Wang Y, Zhao S (2010) Red non-doped electroluminescent dyes based on arylamino fumaronitrile derivatives. Dyes Pigments 85:86–92
2. Giovanella U, Botta C, Bossi A, Licandro E, Maiorana S (2006) Electroluminescent orthofused thiophene dye embedded in polyvinylcarbazole. J Appl Phys 100:83107–83110
3. Hoshimoto M, Igawa S, Yashima M, Kawata I, Hoshino M, Osawa M (2011) Highly efficient green organic light-emitting diodes containing luminescent three-coordinate copper (I) complexes. J Am Chem Soc 133:10348–10351
4. Belfield KD, Hagan DJ, Stryland EWV, Schafer KJC, Negres R (1999) New two-photon absorbing fluorene derivatives: synthesis and nonlinear optical characterization. Org Lett 1:1575–1578
5. Raposo MMM, Sousa AMRC, Kirsch G, Cardoso P, Belsley M, Gomes EM, Fonseca AMC (2006) Synthesis and characterization of dicyanovinyl-substituted thienylpyrroles as new nonlinear optical chromophores. Org Lett 8:3681–3684
6. Verma R, Dhar R, Rath MC, Sarkar SK, Dabrowski R (2012) Electron beam irradiation induced changes in the dielectric and electro-optical properties of a room temperature nematic display material 4-(trans-4′-*N*-hexylcyclohexyl) isothiocyanatobenzoate. J Phys Chem Solids 73:288–295
7. Shimizu M, Hiyama T (2010) Organic fluorophores exhibiting highly efficient photoluminescence in the solid state. Chem Asian J 5:1516–1531
8. Chaskar A, Chen H, Wong K (2011) Bipolar host materials: a chemical approach for highly efficient electrophosphorescent devices. Adv Mater 23:3876–3895
9. Morandeira A, Fürstenberg A, Gumy JC, Vauthey E (2003) Fluorescence quenching in electron-donating solvents 1. Influence of the solute-solvent interactions on the dynamics. J Phys Chem A 107:5375–5383
10. Karpiuk J (2004) Dual fluorescence from two polar excited states in one molecule structurally additive photophysics of crystal violet lactone. J Phys Chem A 108:11183–11195
11. Kang H, Facchetti A, Jiang H, Cariati E, Righetto S, Ugo R, Zuccaccia C, Macchioni A, Stern CL, Liu Z, Ho ST, Brown EC, Ratner MA, Marks TJ (2007) Ultralarge hyperpolarizability twisted π-electron system electro-optic chromophores: synthesis solid-state and solution-phase structural characteristics electronic structures linear and nonlinear optical properties and computational studies. J Am Chem Soc 129:3267–3286
12. Grazulevicius JV, Strohriegl P, Pielichowski J, Pielichowski K (2003) Carbazole-containing polymers: synthesis properties and applications. Prog Polym Sci 28:1297–1353
13. Shan W, Chang G, Zhu F, Zhang L (2011) Synthesis of carbazoled poly(arylene imino). Adv Mater Res 284–286:1863–1866
14. Wang H, Chen G, Xu X, Chen H, Ji S (2010) The synthesis and optical properties of benzothiazole-based derivatives with various π-electron donors as novel bipolar fluorescent compounds. Dyes Pigments 86:238–248
15. Ouyanga XH, Zenga HP, Ding GY, Jiang WL, Li J (2009) Luminance materials containing carbazole and triphenylamine exhibiting high hole-transporting properties. Synth Met 159:2063–2069
16. Deligeorgiev T, Vasilev A, Kaloyanova S, Vaquero JJ (2010) Styryl dyes–synthesis and applications during the last 15 years. Color Technol 126:55–80
17. Qian Y, Xiao G, Wang G, Sun Y, Cui Y, Yuan C (2006) Solvatochromism of a novel betaine dye derived from purine. Dyes Pigments 71:109–117
18. Qian Y (2008) 3,6-disubstituted carbazole chromophores containing thiazole and benzothiazole units: synthesis characterization and first-order hyperpolarizabilities. Dyes Pigments 76:277–281
19. Yoon KR, Ko SO, Lee SM, Lee H (2007) Synthesis and characterization of carbazole derived nonlinear optical dyes. Dyes Pigments 75:567–573
20. Huang X, Zhong S, Yan X, Ke X, Srisanit N, Wang MR (2004) The synthesis and nonlinear optical property of carbazole-azo binary compounds. Synth Met 140:79–86
21. Panthi K, Adhikari RM, Kinstle TH (2010) Visible and near IR emitting organic nanoparticles of aromatic fumaronitrile core-based donor–acceptor compounds. J Photochem Photobiol A Chem 215:179–184
22. Song S, Ju D, Li J, Li D, Wei Y, Dong C, Lin P, Shuang S (2009) Synthesis and spectral characteristics of two novel intramolecular charge transfer fluorescent dyes. Talanta 77:1707–1714
23. Sophy KB, Calaminici P, Pal S (2007) Density functional static dipole polarizability and first-hyperpolarizability calculations of Na_n (n=2,4,6,8) clusters using an approximate CPKS method and its comparison with MP2 calculations. J Chem Theory Comput 3:716–727
24. Hu B, Fu SJ, Tao FXT, Zhu HY, Cao KS, Huang W, You XZ (2011) Linear heterocyclic aromatic fluorescence compounds having various donor-acceptor spacers prepared by the combination of carbon-carbon bond and carbon-nitrogen bond cross-coupling reactions. J Org Chem 76:4444–4456
25. Takimoto Y, Isborn CM, Eichinger BE, Rehr JJ, Robinson BH (2008) Frequency and solvent dependence of nonlinear optical properties of molecules. J Phys Chem C 112:8016–8021
26. Becke AD (1993) A new mixing of Hartree-Fock and local density–functional theories. J Chem Phys 98:1372–1377
27. Foresman JB, Frisch Æ (1996) Exploring chemistry with electronic structure methods, 2nd edn. Gaussian Inc, Pittsburgh
28. Mennucci B, Cappelli C, Guido CA, Cammi R, Tomasi J (2009) Structures and properties of electronically excited chromophores in solution from the polarizable continuum model coupled to the time-dependent density functional theory. J Phys Chem A 113:3009–3020
29. Petsalakis ID, Georgiadou DG, Vasilopoulou M, Pistolis G, Dimotikali D, Argitis P, Theodorakopoulos G (2010) Theoretical investigation on the effect of protonation on the absorption and emission spectra of two amine-group-bearing red "Push-Pull" emitters 4-dimethylamino-4′-nitrostilbene and 4-(dicyanomethylene)-2-methyl-6-*p*-(dimethylamino) styryl-*4H*-pyran by DFT and TDDFT calculations. J Phys Chem A 114:5580–5587
30. Oliva MM, Casado J, Raposo MMM, Fonseca AMC, Hartmann H, Hernández V, Navarrete JTL (2006) Structure–property relationships in push-pull amino/cyanovinyl end-capped oligothiophenes: quantum chemical and experimental studies. J Org Chem 71:7509–7520
31. Gupta VD, Padalkar VS, Phatangare KR, Patil VS, Umape PG, Sekar N (2011) The synthesis and photo-physical properties of

extended styryl fluorescent derivatives of *N*-ethyl carbazole. Dyes Pigments 88:378–384
32. Padalkar VS, Tathe AB, Gupta VD, Patil VS, Phatangare KR, Sekar N (2012) Synthesis and photo-physical characteristics of inspired 2-substituted benzimidazole, benzoxazole and benzothiazole fluorescent derivatives. J Fluoresc 22:311–322
33. Patil VS, Padalkar VS, Phatangare KR, Gupta VD, Umape PG, Sekar N (2012) Synthesis of new ESIPT-fluorescein: photophysics of pH sensitivity and fluorescence. J Phys Chem A 116:536–545
34. Mataga N, Kaifu Y, Koizumi M (1956) Solvent effects upon fluorescence spectra and the dipole moments of excited molecules. Bull Chem Soc Jpn 29:465–470
35. Lippert E (1957) Spektroskopische bestimmung des dipolmomentes aromatischer verbindungen im ersten angeregten singulettzustand. Z Elektrochem 61:962–975
36. Mataga N (1963) Solvent effects on the absorption and fluorescence spectra of naphthylamines and isomeric aminobenzoic acids. Bull Chem Soc Jpn 36:654–662
37. Mataga N, Kaifu Y, Koizumi M (1955) The solvent effect on fluorescence spectrum change of solute-solvent interaction during the lifetime of excited solute molecule. Bull Chem Soc Jpn 28:690–691
38. Lakowicz JR (1999) Principles of fluorescence spectroscopy, 2nd edn. Kluwer, New York
39. Reichardt C (1994) Solvatochromic dyes as solvent polarity indicators. Chem Rev 94:2319–2358
40. Bakhshiev NG (1964) Universal intermolecular interactions and their effect on the position of the electronic spectra of molecules in two component solutions. Opt Spektrosk 16:821–832
41. Kawski A (1966) der Wellenzahl von Elecktronenbanden Lumineszierenden Moleküle. Acta Phys Polon 29:507–518
42. Chamma A, Viallet PCR (1970) Determination du moment dipolaire d'une molecule dans un etat excite singulet. Acad Sci Ser C 270:1901–1904
43. Kawski A (1964) Dipol momente einiger naphthole im grund- und anregungszustand. Naturwissenschaften 51:82–83
44. Jose J, Burgess K (2006) Syntheses and properties of water-soluble nile red derivatives. J Org Chem 71:7835–7839
45. Frisch MJ, Trucks GW, Schlegel HB, Scuseria GE, Robb MA, Cheeseman JR, Scalmani G, Barone V, Mennucci B, Petersson GA, Nakatsuji H, Caricato M, Li X, Hratchian HP, Izmaylov AF, Bloino J, Zheng G, Sonnenberg JL, Hada M, Ehara M, Toyota K, Fukuda R, Hasegawa J, Ishida M, Nakajima T, Honda Y, Kitao O, Nakai H, Vreven T, Montgomery JA Jr, Peralta JE, Ogliaro F, Bearpark M, Heyd JJ, Brothers E, Kudin KN, Staroverov VN, Kobayashi R, Normand J, Raghavachari K, Rendell A, Burant JC, Iyengar SS, Tomasi J, Cossi M, Rega N, Millam NJ, KleneM Knox JE, Cross JB, Bakken V, Adamo C, Jaramillo J, Gomperts R, Stratmann RE, Yazyev O, Austin AJ, Cammi R, Pomelli C, Ochterski JW, Martin RL, Morokuma K, Zakrzewski VG, Voth GA, Salvador P, Dannenberg JJ, Dapprich S, Daniels AD, Farkas O, Foresman JB, Ortiz JV, Cioslowski J, Fox DJ (2010) Gaussian 09 revision C01. Gaussian Inc, Wallingford
46. Treutler O, Ahlrichs R (1995) Efficient molecular numerical integration schemes. J Chem Phys 102:346–354
47. Lee C, Yang W, Parr RG (1988) Development of the Colle-Salvetti correlation-energy formula into a functional of the electron density. Phys Rev B 37:785–789
48. Hehre WJ, Radom L, Schleyer PR, Pople J (1986) Ab Initio molecular orbital theory. Wiley, New York
49. Bauernschmitt R, Ahlrichs R (1996) Treatment of electronic excitations within the adiabatic approximation of time dependent density functional theory. Chem Phys Lett 256:454–464
50. Furche F, Rappaport D (2005) Density functional theory for excited states: equilibrium structure and electronic spectra. In: Olivucci M (ed) Computational photochemistry, vol 16 chapter 3. Elsevier, Amsterdam
51. Valeur B (2001) Molecular fluorescence: principles and applications. Wiley-VCH Verlag, Weinheim
52. Cossi M, Barone V, Cammi R, Tomasi J (1996) Ab initio study of solvated molecules: a new implementation of the polarizable continuum model. Chem Phys Lett 255:327–335
53. Tomasi J, Mennucci B, Cammi R (2005) Quantum mechanical continuum solvation models. Chem Rev 105:2999–3094
54. Legault CY (2009) CYLview 1 0b. Université de Sherbrooke (http://www.cylview.org)
55. Dennington R, Keith T, Millam J (2009) GaussView version 5. Semichem Inc, Shawnee Mission
56. Ravi M, Samanta A, Radhakrishnan TP (1994) Excited state dipole moments from an efficient analysis of solvatochromic stokes shift data. J Phys Chem 98:9133–9136
57. Aaron JJ, Maafi M, Kersebet C, Parkanyi C, Antonious MS, Motohashi N (1996) A solvatochromic study of new benzo[a]phenothiazines for the determination of dipole moments and specific solute-solvent interactions in the first excited singlet state. J Photochem Photobiol A 101:127–136
58. Kumar S, Rao VC, Rastogi RC (2001) Excited-state dipole moments of some hydroxycoumarin dyes using an efficient solvatochromic method based on the solvent polarity parameter E_T^N. Spectrochim Acta A 57:41–47
59. Harbison GS (2002) Excited state dipole moments from an efficient analysis of solvatochromic stokes shift data. J Am Chem Soc 124:366–367
60. Inamdar SR, Nadaf YF, Mulimani BG (2003) Ground and excited state dipole moments of exalite 404 and exalite 417 UV laser dyes determined from solvatochromic shifts of absorption and fluorescence spectra. J Mol Struct 624:47–51
61. Párkányi C, Stem-Beren MR, Martínez OR, Aaron JJ, Bulaceanu-MacNair M, Arrieta AF (2004) Solvatochromic correlations and ground- and excited-state dipole moments of curcuminoid dyes. Spectrochim Acta A 60:1805–1810
62. Masternak A, Wenska G, Milecki J, Skalski B, Franzen S (2005) Solvatochromism of a novel betaine dye derived from purine. J Phys Chem A 109:759–766
63. Nemkovich NA, Pivovarenko VG, Baumann W, Rubinov AN, Sobchuk AN (2005) Dipole moments of 4′-aminoflavonol fluorescent probes in different solvents. J Fluoresc 15:29–36
64. Raikar US, Renuka CG, Nadaf YF, Mulimani BG, Karguppikar AM (2006) Rotational diffusion and solvatochromic correlation of coumarin 6 laser dye. J Fluoresc 16:847–854
65. Jozefowicz M, Heldt JR, Heldt J (2007) Dipole moments studies of fluorenone and 4-hydroxyfluorenone. Spectrochim Acta A 67:316–320
66. Sharma N, Jain SK, Rastogi RC (2007) Solvatochromic study of excited state dipole moments of some biologically active indoles and tryptamines. Spectrochim Acta A 66:171–176
67. Nowak K, Wysocki S (2008) An experimental and theoretical study of dipole moments of *N*-[4-(9-acridinylamino)-3-methoxyphenyl]methane sulfonamide. Spectrochim Acta A 70:805–810
68. Biradar DS, Siddlingeshwar B, Hanagodimath SM (2008) Estimation of ground and excited state dipole moments of some laser dyes. J Mol Struct 875:108–112
69. Reichardt C (2003) Solvent and solvent effects in organic chemistry. Third and enlarged edition. Wiley VCH Verlag GmbH & Co KGaA, Weinheim
70. Suppan P (1983) Excited-state dipole moments from absorption/fluorescence solvatochromic ratios. Chem Phys Lett 94:272–275
71. Stalin T, Rajendiran N (2006) Intramolecular charge transfer associated with hydrogen bonding effects on 2-aminobenzoic acid. J Photochem Photobiol A Chem 182:137–150

72. Rurack K, Bricks JL, Schulz B, Maus M, Reck G, Resch-Genger U (2000) Diphenyl-3-benzothiazol-2-yl-Δ2-pyrazolines: synthesis X-ray structure photophysics and cation complexation properties. J Phys Chem A 104:6171–6188
73. Barto RR Jr, Frank CW, Bedworth PV, Ermer S, Taylor RE (2004) Near-infrared optical absorption behavior in high-β nonlinear optical chromophore-polymer guest-host materials. 1 continuum dielectric effects in polycarbonate hosts. J Phys Chem B 108:8702–8715
74. Kodali G, Kistler KA, Narayanan M, Matsika S, Stanley RJ (2010) Change in electronic structure upon optical excitation of 8-vinyladenosine: an experimental and theoretical study. J Phys Chem A 114:256–267
75. Burke K, Riccardi C, Buthelezi T (2012) Thermosolvatochromism of nitrospiropyran and merocyanine free and bound to cyclodextrin. J Phys Chem B 116:2483–2491
76. Moon IK, Kim N (2009) The synthesis, electrochemical and theoretical nonlinear optical properties of push-pull chromophores for photorefractive composites. Dyes Pigments 82:322–328
77. Sissa C, Parthasarathy V, Drouin-Kucma D, Werts MHV, Blanchard-Desce M, Terenziani F (2010) The effectiveness of essential-state models in the description of optical properties of branched push-pull chromophores. Phys Chem Chem Phys 12:11715–11727
78. Kleinman DA (1962) Nonlinear dielectric polarization in optical media. Phys Rev 162:1977–1979